Journal of Materials Chemistry C

Supporting Information:

Using a mixed ionic electronic conductor to build an analog memristive device with neuromorphic programming capabilities

Klaasjan Maas, Edouard Villepreux, David Cooper, Carmen Jimenez, Hervé Roussel, Laetitia Rapenne, Xavier Mescot, Quentin Rafhay, Michel Boudard, Mónica Burriel*

In order to obtain stoichiometric L2NO4 thin films the La/Ni ratio of the precursor solution, the deposition temperature and number of pulses were first optimized. The optimal growth conditions for L2NO4 thin films are summarized in **Table S1**. Using these conditions, it was possible to grow highly oriented films on [1 0 0]-oriented $SrTiO_3$ single crystals.

Table S1: Optimized deposition conditions used for the growth of L2NO4 thin films by PiMOCVD.

Parameter	Value
Precursors	$La(TMHD)_3$ and $Ni(TMHD)_2$ (m-xylene was used as solvent)
Solution concentration	0.02 mol/L (solvent = m-xylene)
Injection frequency	1 Hz
Opening time	2 ms
Number of injected droplets	4000
Evaporation temperature	220°C - 280°C (several heating stages)
Substrate temperature	650°C
Carrier gas	34% Ar (218 sccm) + 66% O2 (418 sccm)
Total pressure inside the reactor	5 Torr

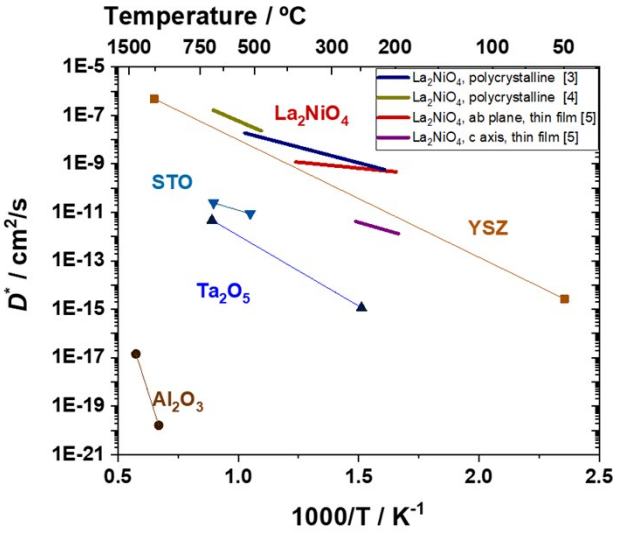

	D*(298 K) cm^2/s	Charac. Diff. Length (nm) (298 K, 600 s)	Charac. Diff. Length (nm) (298 K, 3600 s)
YSZ [1]	$3.82\ 10^{-20}$	0.10	$2.34\ 10^{-1}$
Al_2O_3 [1]	$4.72\ 10^{-104}$	$1.06\ 10^{-43}$	$2.61\ 10^{-43}$
Ta_2O_5 [1]	$2.31\ 10^{-26}$	$7.45\ 10^{-5}$	$1.82\ 10^{-4}$
$SrTiO_3$ [2]	$1.51\ 10^{-18}$	0.60	1.48
La_2NiO_4-poly [3]	$1.66\ 10^{-14}$	63.19	$1.55\ 10^{2}$
La_2NiO_4-poly [4]	$4.13\ 10^{-18}$	1.00	2.44
La_2NiO_4-*ab*-thin film [5]	$1.01\ 10^{-11}$	1556	$3.8\ 10^{3}$
La_2NiO_4-*c*-thin film [5]	$1.86\ 10^{-17}$	2.11	5.18

$\sqrt{4D_i t}$ *is the characteristic diffusion length*

Figure S1: Comparison of the oxygen-tracer diffusion coefficient D* for several oxide materials used in the resistive switching community and known for their VCM-type resistance-change mechanism (such as Ta_2O_5 [1]Al_2O_3 [1] and $SrTiO_3$ [2]). Yttria-stabilized zirconia (YSZ, with the general formula $Zr_{1-x}Y_xO_{2-\delta}$) [1], which enables oxygen ion conduction while blocking electronic conduction, is the most common electrolyte material used in Solid Oxide Fuel Cells (SOFCs). L2NO4 [4,5] has - to date - not received much attention in the memristor community. This is surprising when considering its potential oxygen conduction capabilities all the way down to room temperature.

References:

[1] R. A. De Souza, in Resist. Switch., Wiley-VCH Verlag GmbH & Co. KGaA, Weinheim, Germany, 2016, pp. 125–164.

[2] R. A. De Souza, V. Metlenko, D. Park, T. E. Weirich, Phys. Rev. B 2012, 85, 174109.

[3] R. Sayers, R. A. De Souza, J. A. Kilner, S. J. Skinner, Solid State Ionics 2010, 181, 386.

[4] S. J. Skinner, J. A. Kilner, Solid State Ionics 2000, 135, 709.

[5] M. Burriel, G. Garcia, J. Santiso, J. A. Kilner, R. J. Chater, S. J. Skinner, J. Mater. Chem. 2008, 18, 416.

Figure S2 shows the O and Ti chemical profiles taken below a Pt and a Ti electrode in a Pt/L2NO4/Ti memristive device. The intensities are normalized to the STO substrate which contains both O and Ti in a 1:3 ratio. It is interesting to see that the overall amount of oxygen present in the L2NO4 film seems lower below Ti than below Pt, indeed suggesting that Ti has scavenged oxygen from L2NO4. Furthermore, the oxygen peak present at the Ti/L2NO4 interface coexists with a high intensity of Ti. When considering the normalized intensities at a distance of $d \simeq 100$ nm, a Ti/O ratio of 1.75/3 can be calculated, which corresponds roughly to the composition $TiO_{1.7}$ (or TiO_{2-y} with $y \simeq 0.3$ the number of oxygen vacancies per unit cell of TiO_2). This calculation is a first approximation as other elements that were not measured could also be present in the interlayer. In addition, this interlayer is probably amorphous, meaning that the composition can largely vary depending on the location and could for example take the form of a chemical gradient between the Ti electrode and the L2NO4 film (as Ti is being oxidized by L2NO4). The presence of a highly oxygen deficient TiO_{2-y} is plausible, meaning that the interlayer would rather be an n-type semiconductor than an insulator.

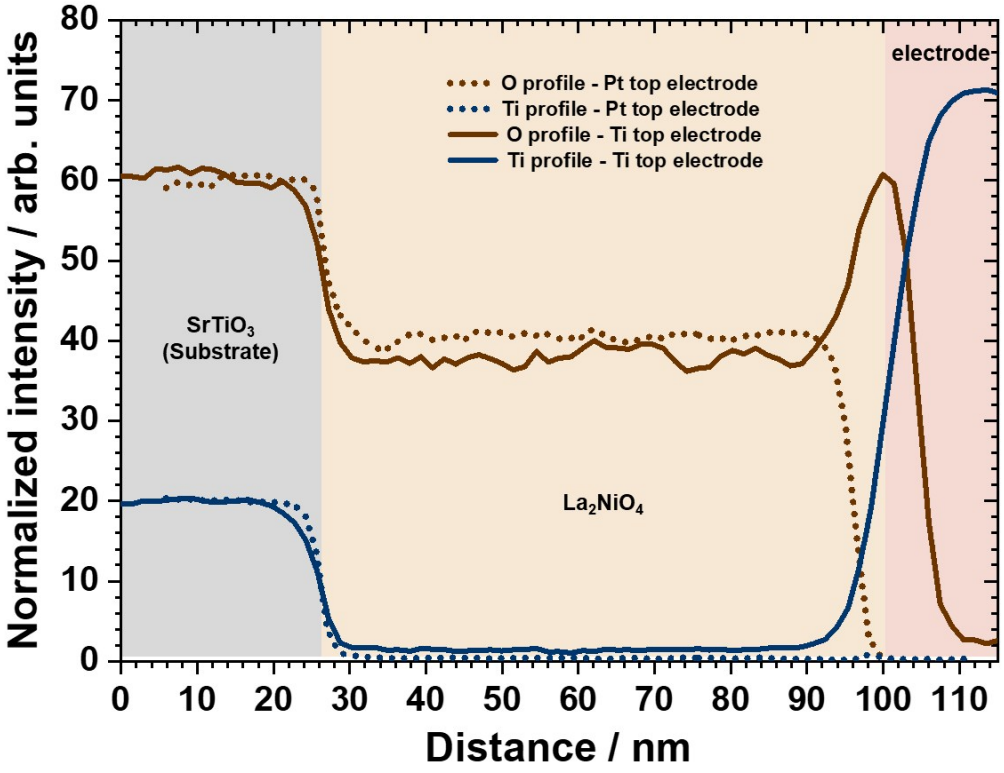

Figure S2: Comparison between the two Pt/L2NO4/STO and Ti/L2NO4/STO heterostructures. A clear oxygen peak is present at the L2NO4/Ti interface and extends about 8 nm into the Ti electrode, suggesting a TiO_{2-y} ($y \simeq 0.3$) interlayer has formed at this location.

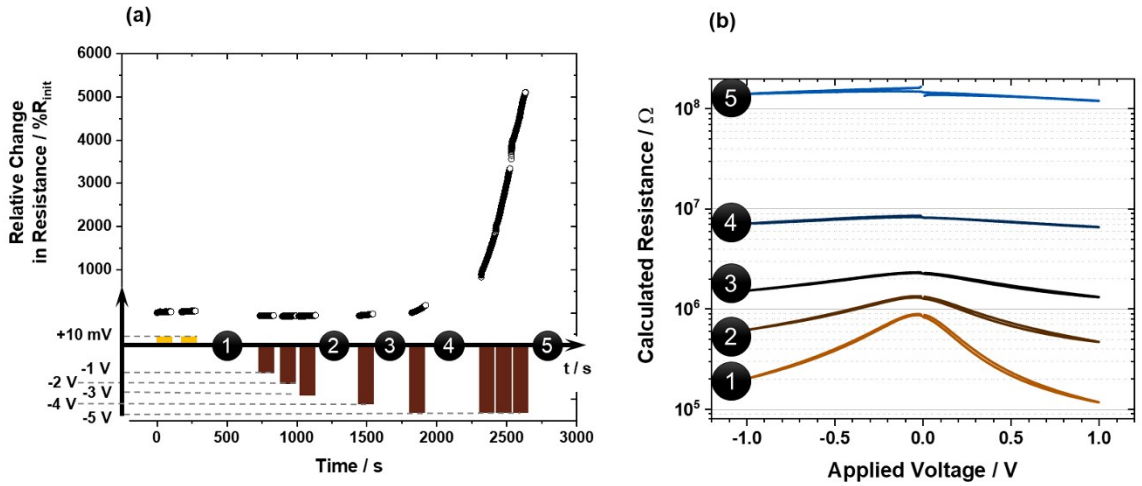

Figure S3: Response of a Pt/L2NO4/Ti device to increasing voltage pulses. (a) Applied voltage over time (2x100 s at +10 mV followed by 100 s at -1 V, -2 V, -3 V, -4 V, -5 V and finally 2x100 s at -5 V again) (b) Evolution of the R-V characteristics (log scale) of the device at different stages of the experiment, these stages are indicated by the numerals in the R(t) sampling curve.

Description of Figure S4: The first five sweeps between ±1 V show ohmic-like I-V characteristics with almost no rectification, suggesting that we are still in the sub-threshold voltage region of the I(V) curve. Already at ±2 V hysteretic and rectifying I-V characteristics start to appear. Interestingly, the current levels and rectification of the device increases with the number of cycles without needing to increase the maximum voltage amplitude nor the dwell time at each voltage step. This suggests that an additional dynamic relaxation in which both the HRS and the LRS are decreasing over time is superimposed to each I(V) cycle. This effect is very clear when cycling at ±3 V where an hysteresis is now visible on both sides of the I(V) curve. At ±4 V, the relaxation is still present, but when cycling ±5 V the device shows two stable and highly reproducible resistance states separated by roughly one order of magnitude.

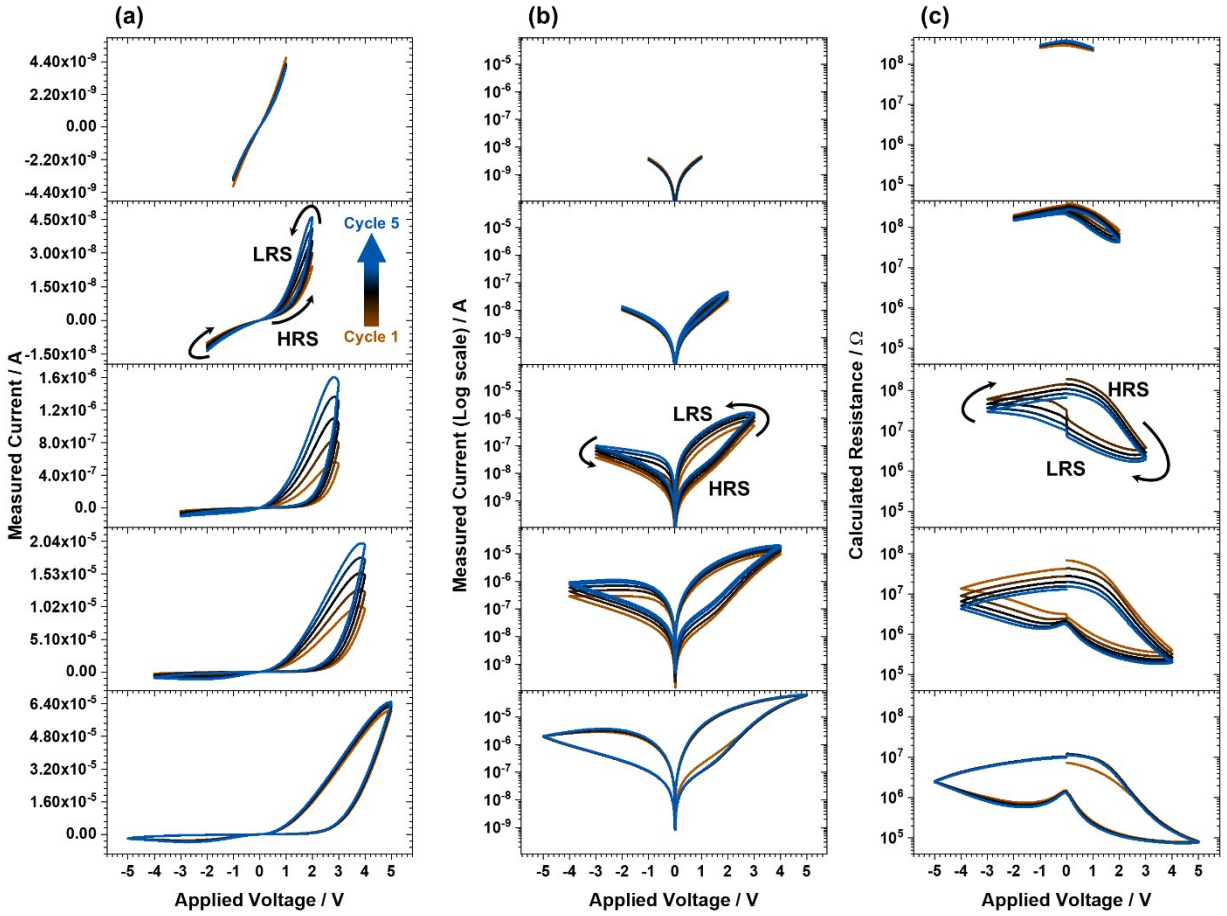

Figure S4: (a) I-V characteristics of a Pt/L2NO4/Ti device after the biasing experiment described in Figure 3.a. Each panel shows five consecutive bipolar I(V) sweeps executed in the same biasing conditions (0 V → +Vmax → 0 V → -Vmax → 0 V). The maximum voltage amplitude (Vmax) is increased from 1 V to 5 V with a step of 1 V in each new panel. (b) is the same as (a) but in semilogY scale and (c) is the same as (b) but described in terms of R-V characteristics. The Pt electrode was biased while Ti remained grounded throughout the experiment.

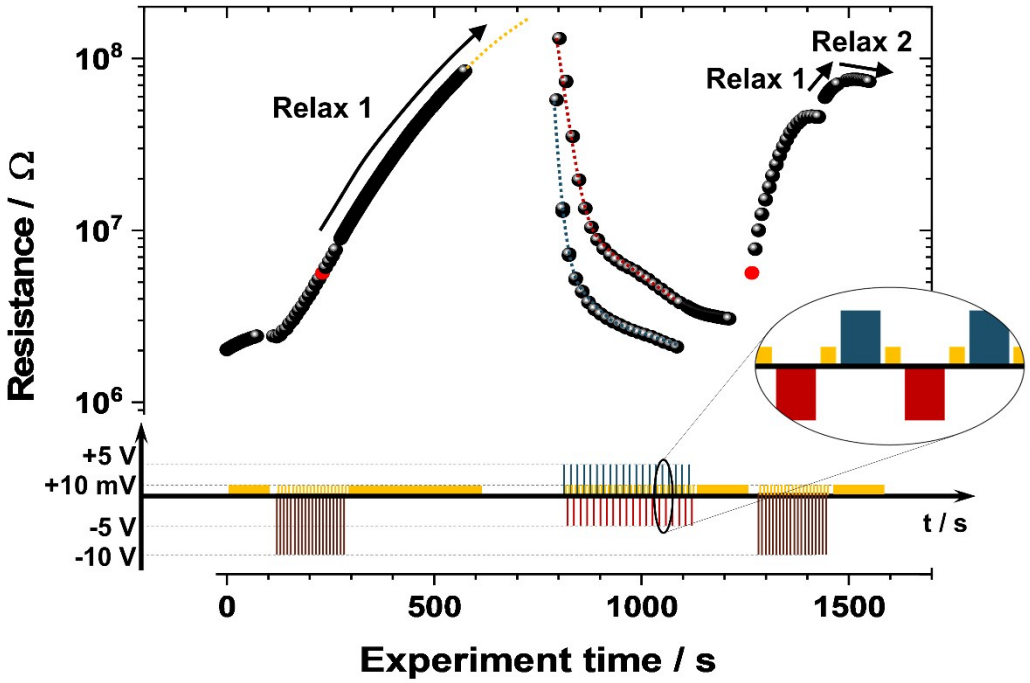

Figure S5: Evolution of the resistance (same data as Figure 3b but in log scale) over time showing the history dependance of the Pt/L2NO4/Ti memristive device. Only the readouts at +10 mV are represented. The red points correspond to two states with the same resistance value (5.6×10^6 Ω) and for which identical pulses [-10 V; 1500 ms] result in a larger resistance increase the second time the train of pulses is applied.

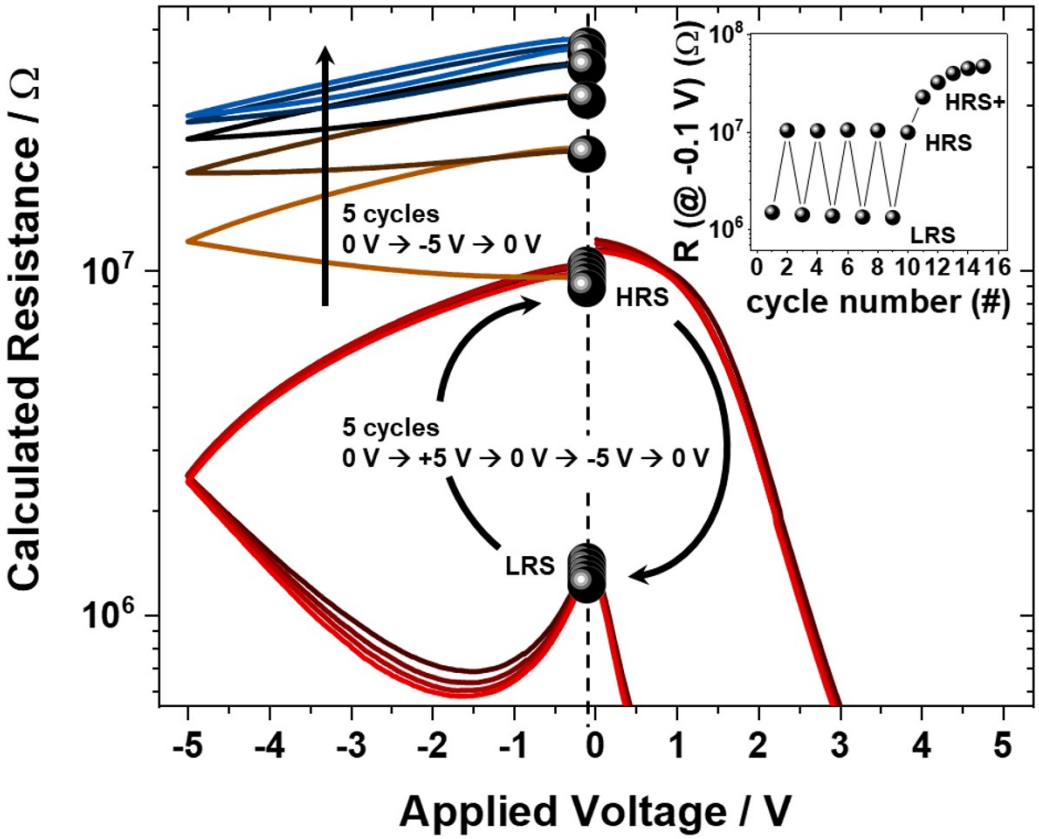

Figure S6: R-V characteristics of a Pt/L2NO4/Ti device showing highly reproducible HRS and LRS over five consecutive ±5 V cycles. The device is then gradually programmed to an even higher resistance state (HRS+) when carrying out five unipolar 0 V → -5 V → 0 V voltage sweeps. The inset shows the resistance state of the device (read out at -100 mV) after each cycle.